IEEE INFOCOM 2023 - IEEE Conference on Computer Communications Workshops (INFOCOM WKSHPS) | 978-1-6654-9427-4/23/$31.00 ©2023 IEEE | DOI: 10.1109/INFOCOMWKSHPS57453.2023.10225988

WiWm-EP: Wi-Fi CSI-based Wheat Moisture Detection Using Equivalent Permittivity

Pengming Hu[a], †Weidong Yang[a], ΙΙXuyu Wang, ‡Shiwen Mao, and Erbo Shen[a]
[a] Henan Key Laboratory of Grain Photoelectric Detection and Control, Henan University of Technology, Zhengzhou, 450001
†College of Information Science and Engineering, Henan University of Technology, Zhengzhou, 450001, China
ΙΙKnight Foundation School of Computing and Information Sciences, Florida International University, FL 33199, USA
‡Department of Electrical and Computer Engineering, Auburn University, Auburn, AL 36849-5201
Email: hupengming@stu.haut.edu.cn, Yangweidong@haut.edu.cn, xuywang@fiu.edu, smao@ieee.org, shenbo412@163.com

***Abstract*—Moisture content is one of the important indexes of food storage security. The existing detection methods are time-consuming and high cost such that it is difficult to realize on-line moisture detection. In this paper, according to the dielectric properties of wheat, we propose a wheat moisture content detection system with commercial Wi-Fi devices, termed WiWm-EP. First, we introduce the relationship between the moisture content of wheat and its dielectric constant. Then, we establish an equivalent permittivity (EP) model to characterize wheat moisture content, where the EP can be calculated from channel state information (CSI) of the dual antenna model. Besides, we build the fitting function between the EP and the moisture content as the wheat moisture detection model. Finally, we evaluate the performance of the system through different experiments. The average relative error of the detection results of five wheat samples with different moisture contents is less than 3%.**

***Index Terms*—Wireless Sensing, Channel State Information (CSI), Wheat Moisture Detection, Equivalent Permittivity (EP).**

I. Introduction

Recently, the global grain reserves have reached billions of tons [1]. It is particularly important to ensure the security of grain reserves. Grain moisture detection is one of the key technologies in ensuring the security of stored grain [2], [3]. The problems of grain heating, insects, and mildew during storage all depend on the moisture content. For example, when the grain is about to go moldy and deteriorate, the grain moisture will change in advance. If the change of grain moisture can be detected in time and the measurement can be taken, the grain moldiness and deterioration can be avoided. Therefore, an efficient and accurate grain moisture detection technology is very important for guaranteeing grain security.

The traditional moisture detection technology is mainly based on the drying method, but this method is very time-consuming and destroys the grain itself. Recent methods (e.g., electrical resistance [4], near-infrared spectroscopy [5], and hyperspectral spectroscopy [6]) provide effective solutions for grain moisture detection. Compared with the traditional drying method, these approaches have the advantages of high efficiency and no damage to the grain itself. However, these devices are not widely employed because of their high cost.

Due to the rapid development of wireless sensor technologies in Internet of Things (IoT), low-cost and high-precision wireless sensing systems (e.g., Wi-Wheat [1], Wi-Wheat+ [7], and Deep-WMD [8]) have been explored using commodity Wi-Fi devices to detect grain moisture. Similarly, the Wi-Fruit [9] system is also developed for detecting the fruit moisture. However, these systems are based on machine learning methods, which need to update the training weights in a new scenario, which leads to an additional workload. By contrast, in this paper, we exploit the dielectric properties of grains with the wireless sensor theory to achieve the efficient and low-cost grain moisture detection through a pure mathematical model.

In particular, we propose a wheat moisture detection system based on commercial Wi-Fi signals, termed WiWm-EP. First, we introduce the relationship between the moisture content of wheat and its dielectric constant. Because the dielectric constant of wheat will increase with the increase of the moisture content, the moisture content of wheat can be obtained indirectly through the dielectric constant. Traditionally, vector network analyzer (VNA) can be used to measure accurate and stable dielectric constant, but it has a high cost. Therefore, we establish an equivalent permittivity (EP) model to characterize wheat moisture content, and calculate the EP based on the channel state information (CSI) in the dual antenna model of commercial Wi-Fi devices. Meanwhile, to ensure the effectiveness of the WiWm-EP system, we design the preprocessing scheme to eliminate the noise in the raw CSI data. Besides, we establish the fitting function between the EP and the moisture content as the wheat moisture detection model. Finally, we evaluate the system through experiments, where five different wheat moisture contents are used to evaluate the effectiveness of the WiWm-EP system. The results show that the average relative error of the detection results of five wheat samples with different moisture contents is less than 3%. In addition, we also analyze the impact factor on the system.

The main contributions of this paper are summarized below:

- To the best of our knowledge, this is the first work to use Wi-Fi devices to establish an EP model for grain moisture content detection, which provides a theoretical basis for contactless wheat moisture sensing.
- We propose a wheat moisture content detection system based on dielectric properties. This system does not require machine learning methods, thus eliminating the

Authorized licensed use limited to: Auburn University. Downloaded on October 05,2023 at 15:34:47 UTC from IEEE Xplore. Restrictions apply.

978-1-6654-9427-4/23/$31.00 ©2023 IEEE

dependence on a large amount of data and improving the detection efficiency. Besides, we design the preprocessing scheme for the raw CSI data to ensure the effectiveness of the system.

- We evaluate the performance of the system through experiments. The results show that the average relative error of the system is less than 3%.

II. PRELIMINARIES

A. Grain Moisture Detection

Grain moisture detection technology is generally classified into two categories (i.e., the destructive moisture detection method and the non-destructive moisture detection method) [1]. First, the destructive moisture detection method refers to the heating and drying techniques. The principle is to heat and dry the grain sample at a specific temperature, completely evaporate the internal moisture of the sample, and then weigh the mass difference before and after heating to calculate the moisture content of the grain sample. Second, there are many non-destructive moisture detection methods. They mainly include resistance-based, infrared-based, acoustic-based, and microwave-based [1]. These methods indirectly calculate the moisture content of grain through different principles. These methods have the advantages of fast detection speed and no damage to the grain itself. However, high-cost and complex instruments limit the popularity of these methods.

B. Dielectric Constant of Medium

When an electromagnetic wave penetrates through a medium in the free space propagation, the amplitude attenuation coefficient of the electromagnetic wave is $e^{-K_I d}$ and the phase change is $K_R d$ [10], where d is the propagation distance. Specifically, K_R and K_I are defined by,

$$K_R = \omega\sqrt{\varepsilon\mu}\left[\frac{1}{2}\left(\sqrt{1+\frac{\sigma^2}{\omega^2\varepsilon^2}}+1\right)\right]^{1/2}, \quad (1)$$

$$K_I = \omega\sqrt{\varepsilon\mu}\left[\frac{1}{2}\left(\sqrt{1+\frac{\sigma^2}{\omega^2\varepsilon^2}}-1\right)\right]^{1/2}, \quad (2)$$

where ω is the angular frequency of the wave. ε, μ, and σ are dielectric constant, permeability, and conductivity of the medium, respectively. Besides, the dielectric constant can be expressed by $\varepsilon = \varepsilon' + j\varepsilon''$, where the real part ε' is the ability of the medium to store electromagnetic energy, and the imaginary part ε'' is the ability to lose electromagnetic energy. Fig. 1 and Fig. 2 show the relationship between the dielectric constant (i.e., the real part ε' and the imaginary part ε'') and different moisture contents operating in the frequency range from 5 GHz to 6.5 GHz. We can see that the real part ε' and the imaginary part ε'' increases with the increase of moisture content. As the increase of the frequency for a fixed moisture content, the real part ε' will decrease, while the imaginary part ε'' will increase. These results confirm that the dielectric constant is closely related to the moisture content and wireless frequency.

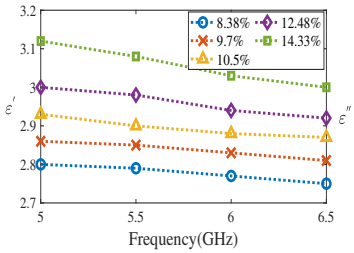

Fig. 1. ε' of wheat with different moisture contents.

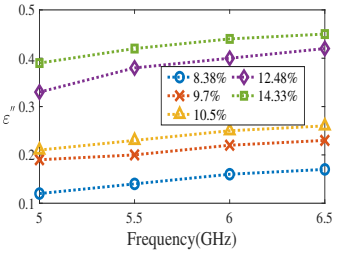

Fig. 2. ε'' of wheat with different moisture contents.

C. Wi-Fi CSI Sensing

The received Wi-Fi signal after penetrating through the medium can be modeled by,

$$A_r \cdot e^{\phi_r} = A_0 e^{-K_I d} \cdot e^{j(K_R d+\theta_0)}, \quad (3)$$

where A_0 and θ_0 are amplitude and phase changes caused by Wi-Fi signal propagation in the air multiplied by the initial amplitude and phase, respectively. d is the propagation path distance in the medium. Specifically, the amplitude A_r and phase ϕ_r can be extracted from the commercial W-iFi network interface cards (NICs). The commercial Wi-Fi physical layer (PHY) adopts an orthogonal frequency-division multiplexing (OFDM) technology, where the device can report CSI data in the frequency domain [11]. Wi-Fi CSI over different subcarriers can be expressed by $\mathrm{H} = (\mathrm{H}(f_1), \mathrm{H}(f_2) \ldots \mathrm{H}(f_k))$, where k is the number of subcarriers. The CSI of the k_{th} subcarrier is specifically defined by,

$$H_k = |H_k| e^{j\angle H_k}, \quad (4)$$

where $|H_k|$ is the amplitude and $\angle H_k$ is the phase.

In fact, the dielectric constant is a complex number, which is difficult to obtain from the Wi-Fi sensing system. Thus, we leverage the EP related to K_R and K_I, and calculate K_R and K_I based on a dual antenna Wi-Fi signal transmission model.

III. EQUIVALENT PERMITTIVITY MODEL

In this section, we introduce the established EP in detail.

A. Equivalent permittivity model

Since the dielectric constant cannot be directly extracted from the Wi-Fi sensing system, we propose an EP model for grain. The model can effectively build the relationship between grain dielectric constant and moisture content. Details of the model are as follows.

First, we perform the quotient operation on Eq. 1 and Eq. 2 to eliminate the part parameters, which is expressed by,

$$\left(\frac{k_R}{k_I}\right)^2 = \frac{\sqrt{1+\frac{\sigma^2}{\omega^2\varepsilon^2}}+1}{\sqrt{1+\frac{\sigma^2}{\omega^2\varepsilon^2}}-1}. \quad (5)$$

Authorized licensed use limited to: Auburn University. Downloaded on October 05,2023 at 15:34:47 UTC from IEEE Xplore. Restrictions apply.

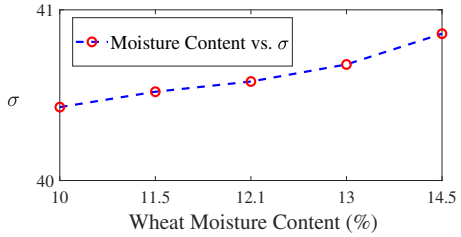

Fig. 3. Electrical conductivity of wheat with different moisture contents.

Next, we transform the values of K_R and K_I into input parameters, and then Eq. 5 is transformed into,

$$\frac{\sigma^2}{\omega^2\varepsilon^2} = \left(\frac{\left(\frac{k_R}{k_I}\right)^2+1}{\left(\frac{k_R}{k_I}\right)^2-1}\right)^2 - 1. \tag{6}$$

Specifically, we analyze Eq. 6 and find that a specific value can be obtained by inputting the values of K_R and K_I. The specific value $\frac{\sigma^2}{\omega^2\varepsilon^2}$ includes the dielectric constant ε and the conductivity σ of the medium and wave angular frequency ω. And $\omega = 2\pi f$, where f is the frequency of the wave. If we keep Wi-Fi working at a fixed frequency, ω can be regarded as a constant. Meanwhile, the conductivity σ of the medium varies with the temperature, and the grain is non-conductive. Thus we approximate the σ to a constant at a room temperature. We then measure the conductivity of wheat with different moisture contents at the room temperature of 23°C. The results in Fig. 3 illustrate that when the moisture content of wheat changes by more than 4%, the corresponding conductivity changes by no more than 2%. In Fig. 1, if the moisture content of wheat changes by more than 4%, the dielectric constant changes by about 9%. Therefore, we believe that the conductivity can be approximated as a constant. Finally, when Wi-Fi works at a fixed frequency, we approximate $\frac{\sigma^2}{\omega^2\varepsilon^2}$ to $\frac{1}{\tilde{\varepsilon}^2}$, where $\tilde{\varepsilon}$ denotes the EP, that is,

$$\tilde{\varepsilon} \approx \sqrt{\frac{1}{\left(\frac{\left(\frac{k_R}{k_I}\right)^2+1}{\left(\frac{k_R}{k_I}\right)^2-1}\right)^2 - 1}} \approx \frac{k_R}{k_I}. \tag{7}$$

It can be seen from Eq. 7 that the EP $\tilde{\varepsilon}$ value only depends on the ratio $\frac{k_R}{k_I}$. In this paper, we leverage $\tilde{\varepsilon}$ to characterize the grain moisture content, and $\tilde{\varepsilon}$ is a real value without an unit.

B. Calculation of K_R and K_I from Wi-Fi sensing

Based on Eq. 3, we design a dual antenna transmission model to calculate K_R and K_I. Specifically, the signal transmitting end is equipped with an antenna, and the signal receiving end is equipped with two receiving antennas. The received signals $A_{r_1} \cdot e^{\phi_{r1}}$ and $A_{r_2} \cdot e^{\phi_{r2}}$ of two adjacent antennas on the same network card after penetrating through the grain can be defined by,

$$\begin{aligned} A_{r_1} \cdot e^{\phi_{r1}} &= A_0 e^{-K_I d_1} \cdot e^{j(K_R d_1 + \theta_0)}, \\ A_{r_2} \cdot e^{\phi_{r2}} &= A_0 e^{-K_I d_2} \cdot e^{j(K_R d_2 + \theta_0)}, \end{aligned} \tag{8}$$

where d_1 and d_2 are the path distance of the Wi-Fi signal in the grain, respectively. As Fig. 4 illustrates, when there is no grain medium, we consider the diameter propagation distance between the transmitting antenna and the two receiving antennas is equal. When the grain exists in line of sight (LOS) between the transmitting antenna and the receiving antenna, Wi-Fi through the grain will cause a refraction effect. Due to the different refraction angles caused by the different directions of the two antennas, the propagation distance changes differently ($d_1 \neq d_2$). In fact, when the grain is present, we first eliminate the parameters A_0 and θ_0 in an unknown air channel through the quotient operation of adjacent antennas and obtain the correlation equations about K_R and K_I. The process is as follows,

$$\frac{A_{r_1} \cdot e^{\phi_{r1}}}{A_{r_2} \cdot e^{\phi_{r2}}} = \frac{A_0 e^{-K_I d_1} \cdot e^{j(K_R d_1 + \theta_0)}}{A_0 e^{-K_I d_2} \cdot e^{j(K_R d_2 + \theta_0)}}. \tag{9}$$

According to Eq. 9, we operate the amplitude and phase respectively. First, the amplitude quotient of adjacent antennas can be expressed by,

$$\frac{A_{r_1}}{A_{r_2}} = \frac{A_0 e^{-K_I d_1}}{A_0 e^{-K_I d_2}} = e^{-K_I(d_1 - d_2)}. \tag{10}$$

Then the equation about K_I is as follows,

$$K_I = \frac{\ln \frac{A_{r_1}}{A_{r_2}}}{d_2 - d_1}. \tag{11}$$

Next, the phase quotient of adjacent antennas can be expressed by,

$$\frac{e^{\phi_{r_1}}}{e^{\phi_{r_2}}} = \frac{e^{j(K_R d_1 + \theta_0)}}{e^{j(K_R d_2 + \theta_0)}}. \tag{12}$$

It can be found that Eq. 12 converts the phase quotient of adjacent antennas into phase difference,

$$\phi_{r_1} - \phi_{r_2} = \Delta\phi_{r_1 - r_2} = K_R(d_1 - d_2). \tag{13}$$

Then the equation about K_R is obtained by,

$$K_R = \frac{\Delta\phi_{r_1 - r_2}}{d_1 - d_2}. \tag{14}$$

It can be seen that the value of K_I is obtained by dividing the amplitude quotient of two adjacent antennas by the distance difference of two antenna propagation paths, and the value of K_R is obtained by dividing the phase difference of two adjacent antennas by the distance difference of two antenna propagation paths. Because the values of d_1 and d_2 are unknown, Eq. 11 and Eq. 14 cannot directly calculate the values of K_I and K_R. However, according to the Eq. 7, we can eliminate d_1 and d_2 by the quotient of Eq. 11 and Eq. 14, that is,

$$\frac{K_R}{K_I} = \frac{\Delta\phi_{r_1 - r_2}}{\cancel{d_1 - d_2}} \cdot \frac{-\cancel{(d_1 - d_2)}}{\ln \frac{A_{r_1}}{A_{r_2}}} = -\frac{\Delta\phi_{r_1 - r_2}}{\ln \frac{A_{r_1}}{A_{r_2}}}. \tag{15}$$

In Eq. 15, we eliminate the unknown parameters (d_1 and d_2) and also ensure the input of the EP model in Eq. 7. It is noticed that the calculated EP is independent of the grain thickness.

Authorized licensed use limited to: Auburn University. Downloaded on October 05,2023 at 15:34:47 UTC from IEEE Xplore. Restrictions apply.

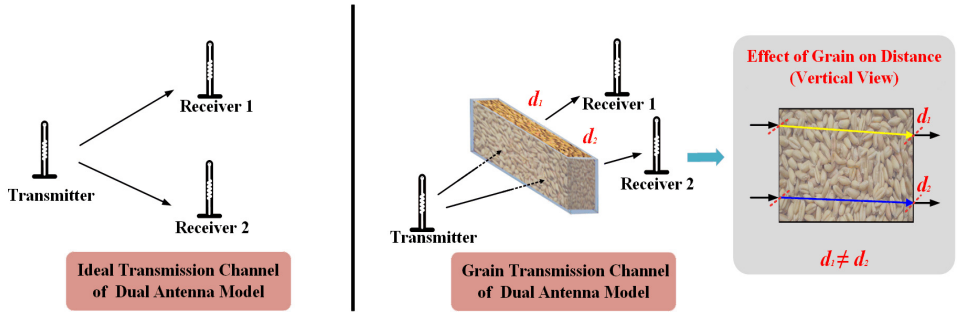

Fig. 4. Dual antenna model for Wi-Fi signal transmission.

IV. THE WIWM-EP SYSTEM DESIGN

In this section, we will introduce the WiWm-EP system design. As shown in Fig. 5, the system architecture includes a CSI data collection module, a CSI preprocessing module, a model establishment module, and a moisture detection module.

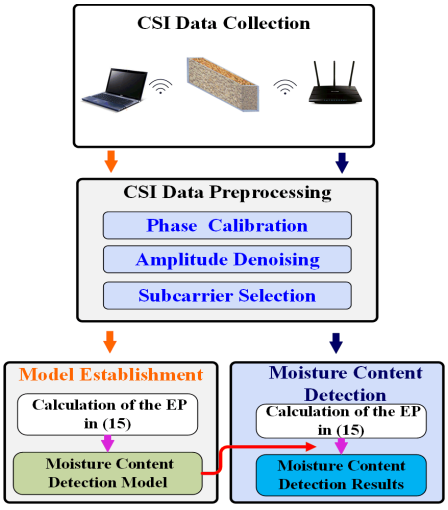

Fig. 5. The system architecture of WiWm-EP.

A. CSI Data Collection

For wheat samples with different moisture contents, we set the same experimental condition for data collection. We collect raw CSI data from wheat samples with five moisture contents in the LOS link through commercial Wi-Fi devices, and then extract CSI amplitude and phase for the moisture content detection.

B. CSI Data Preprocessing

In the data preprocessing stage, we first implement the phase calibration and the amplitude denoising. Then, we select the data with the most stable subcarrier.

CSI Phase Calibration: Due to the asynchronous hardware between transceivers during Wi-Fi transmissions [12], packet boundary delay (PBD), sampling frequency offset (SFO), and carrier frequency offset (CFO) will cause errors in the CSI phase. To solve these errors, we use a linear transformation for the phase calibration. Details are as follows.

Let $\widehat{\phi}_i$ denote the measurement phase of the subcarrier i, which can be expressed by,

$$\widehat{\phi}_i = \phi_i - 2\pi \frac{\eta_i}{M} \Delta t + \beta + N, \tag{16}$$

where ϕ_i is the true phase, η_i is the subcarrier index of the ith subcarrier, M is the total number of subcarriers, Δt is the time delay, β is the phase offset error, and N is the measurement random noise. Δt and β are caused by PBD, SFO and CFO. Except for N, other measurement errors are linearly correlated. We can use the linear transformation to eliminate the influence from Δt and β [13]. First, we define k and b by,

$$\begin{cases} k = \frac{\widehat{\phi_M} - \widehat{\phi_1}}{\eta_M - \eta_1} \\ b = \frac{1}{M} \sum_{i=1}^{M} \widehat{\phi}_i, \end{cases} \tag{17}$$

where k and b represent the slope and the offset of the received phase, respectively. Then the phase can be calibrated by,

$$\begin{aligned} \tilde{\phi}_i &= \widehat{\phi}_i - k\eta_i - b \\ &= \widehat{\phi}_i - \frac{\widehat{\phi_M} - \widehat{\phi_1}}{\eta_M - \eta_1} \cdot \eta_i - \frac{1}{M} \sum_{i=1}^{M} \widehat{\phi}_l. \end{aligned} \tag{18}$$

We can find $\tilde{\phi}_i$ has eliminated the influence of Δt and β, but still containing the noise N. We can exploit a sliding window averaging method to remove the remaining noise. Besides, the cycle range of the collected CSI signal is $[-\pi, \pi]$, and the phase inversion will occur at the critical points $-\pi$ and π. Therefore, we need to unwrap the phase before the linear transformation. Fig. 6 shows the raw phase and the calibrated phase of the wheat sample with 10% moisture content. It can be seen that the phase after the calibration is more smooth and more stable.

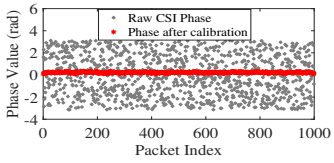

Fig. 6. CSI phase calibration.

CSI Amplitude Denoising: The collected raw CSI amplitude data usually contains irregular multipath noise. As shown

Authorized licensed use limited to: Auburn University. Downloaded on October 05,2023 at 15:34:47 UTC from IEEE Xplore. Restrictions apply.

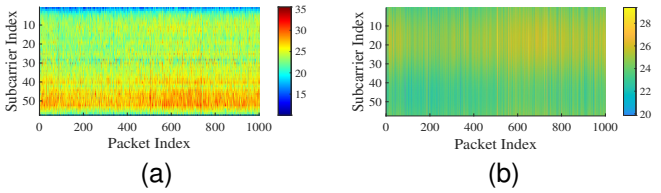

Fig. 7. CSI amplitude denoising ((a) raw amplitude, (b) amplitude after noise removal.)

in Fig. 7a, it is the raw amplitude data of 10% wheat moisture content. To eliminate these noises, we use the the combination of Fourier transform and smoothing filtering. Specifically, we use the CSI amplitude in the frequency domain to obtain the CIR in the time domain through Inverse Fast Fourier Transform (IFFT). In the time domain, the CIR in the first few microseconds is the path signal of the Wi-Fi penetrating grain, which is retained. After removing the path signals of other multipath environments, Fast Fourier Transform (FFT) is performed to obtain the CSI amplitude information of the path where Wi-Fi penetrates grains. Then, we use a smoothing filter to remove other random noises. Finally, the denoising result by using the combination of Fourier transform and smoothing filtering is shown in Fig. 7b. It can be found that the CSI amplitude after multipath noise removal significantly inhibits the multipath.

Subcarrier selection: The impact of indoor multipath environments on the subcarriers of Wi-Fi channel is different, and the smaller variances of subcarriers are usually less affected by the multipath [14], [15]. Thus, our method is to calculate the variance of the calibrated phase for each subcarrier and then select the amplitude and phase data of the subcarrier corresponding to the smallest variance as the "clean" data.

C. Model establishment and moisture content detection

First, we calculate the EP of grain according to Eq. 15 by using the "clean" amplitude and phase data. Then the $\tilde{\varepsilon}$ and moisture content are fitted to obtain the moisture content estimation model. In the moisture content detection stage, we collect the new CSI data, which is processed to calculate the $\tilde{\varepsilon}$ of grain. Finally, we use the established model to detect grain moisture content.

V. EXPERIMENTS AND EVALUATION

In this section, we evaluate the detection performance of WiWm-EP in real environments.

A. Experiment Implementation

Sample Preparation: To ensure the reliability of the WiWm-EP system, we need accurate wheat samples with different moisture contents. We select the same batch of summer wheat in a certain area as the sample material, and the original moisture content is 10%. Then we prepare four wheat samples with different moisture contents according to the same standard (i.e., 100g wheat with 1g water). We use a professional mixer (as shown in Fig. 8) to make the wheat absorb water evenly. Then we seal all wheat samples in bags and let them stand in a refrigerator with the room temperature of 5°C for three months. After three months, we take out the wheat samples with the stable moisture content. Then, the moisture of wheat samples is calibrated by an oven drying method to obtain the accurate and real moisture of wheat, where we use a halogen moisture meter, as shown in Fig. 8. Finally, we obtain wheat samples with different moisture contents in Table I.

TABLE I
THE STATE OF WHEAT SAMPLES.

Samples	1	2	3	4	5
Wheat Moisture	10%	11.5%	12.1%	13%	14.5%

Hardware and Software: The hardware of the WiWm-EP system consists of two Lenovo thinkpadx201 notebook computers equipped with Intel 5300 NIC. The first computer is externally connected with one antenna as the signal transmitter, and the other is externally connected with two antennas as the signal receiver. A 1×2 dual antenna communication scheme is formed, and the working frequency is fixed at 5.2 GHz with a bandwidth of 20MHz. In terms of the software, both laptops run Ubuntu Linux14.04 operating system and use the Picosense platform [16] to control CSI data collection. The data processing is carried out on MATLAB 2021b.

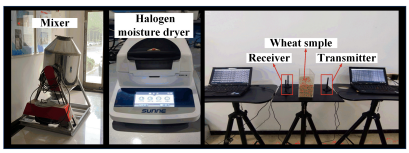

Fig. 8. Wheat sample preparation tool and implementation scenario.

Experimental Setup: The experimental setup of WiWm-EP is shown in Fig. 8. Wheat samples with different moisture contents in the middle of the LOS link are placed in the device made of acrylic material, and we then start to collect CSI data. In the model establishment stage, for wheat samples with moisture contents, CSI data packets are collected for the first time. The transmitter is set to transmit 100 data packets every 1s, with a duration of 10s. A total of 1000 data packets are used for the model establishment. In the stage of moisture content detection, when CSI data is newly collected, the transmitter is set to 100 packets per second for a duration of 1s, and a total of 100 packets are used for moisture content detection.

B. Model Establishment and Overall Performance

Model Establishment: We select the "clean" amplitude and phase data of the 33rd subcarrier to calculate $\tilde{\varepsilon}$. To improve the stability of the model, we use the mean of the 33rd subcarrier phase and amplitude data in 1000 packets to calculate $\tilde{\varepsilon}$. We calculate the $\tilde{\varepsilon}$ of different wheat samples, which is shown as blue points in Fig. 9. It can be found that with the increase of wheat moisture content, the corresponding value of $\tilde{\varepsilon}$ increases. This trend is consistent with the dielectric

Authorized licensed use limited to: Auburn University. Downloaded on October 05,2023 at 15:34:47 UTC from IEEE Xplore. Restrictions apply.

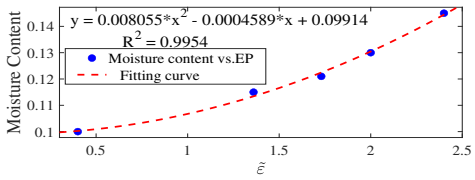

Fig. 9. Fitting curve between $\tilde{\varepsilon}$ and moisture content of Wheat.

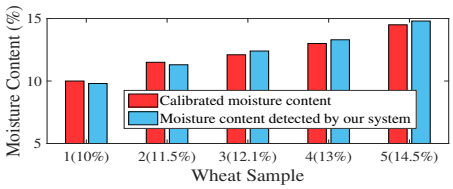

Fig. 10. Results of wheat moisture content detection by WiWm-EP system.

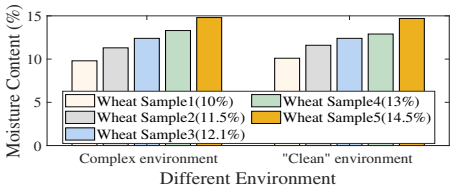

Fig. 11. Results of different environments.

constant of the wheat itself, which verifies the effectiveness of the EP. Then, the $\tilde{\varepsilon}$ and moisture content are fitted to obtain the wheat moisture content detection model. As shown in the red curve in Fig. 9, we have obtained the moisture content detection model of wheat, where R^2 represents the closeness between the fitting curve and the data. The closer it is to 1, the better the fitting effect. The model $R^2 = 0.9954$.

Overall Performance: We collect new CSI data from different wheat samples and detect the moisture content through the WiWm-EP system. Fig. 10 shows the moisture content detection results. The red bar graph is the calibrated moisture content. The blue bar chart is the moisture content detected by the WiWm-EP system. Specifically, the moisture content of wheat samples detected by our system is 9.8%, 11.3%, 12.4%, 13.3%, and 14.8%, respectively. In term of the calibrated moisture contents (i.e., the ground truths), we can obtain the relative errors with 2%, 1.7%, 2.5%, 2.3%, and 2.1%, respectively. The average relative error of our system is 2.1%.

Meanwhile, we change the environment for data collection. We collect CSI data in a clean indoor environment. The results are shown in Fig. 11. The moisture content detection results of wheat in the "clean" environment are 10.1%, 11.6%, 12.4%, 12.9%, and 14.7%, respectively. The relative errors are 1%, 0.8%, 2.5%, 0.8%, and 1.4%, respectively and the average relative error of the system is 1.3%. The average relative error of our system in different environments is less than 3%. Thus, our system can effectively remove the environment noise.

VI. CONCLUSIONS

In this paper, we proposed a wheat moisture detection system based on commercial Wi-Fi devices, called WiWm-EP. Specifically, we built the relationship between the moisture content of wheat and the dielectric constant, and developed an EP model to detect the moisture content of grains. The experimental results showed that the average relative error of our system was less than 3%, which validated the effectiveness of our proposed system.

VII. ACKNOWLEDGMENTS

This work is supported in part by the National Science Foundation of Henan (No.222300420004) and Major Public Welfare Special Projects of Henan Province (No.201300210100), National Natural Science Foundation of China (No. 62172141, 61772173), the NSFC (61741107), the NSF (CNS-2107190, CNS-2105416, CNS-2321763, and CNS-2107164)), and by the Wireless Engineering Research and Education Center at Auburn University.

REFERENCES

[1] W. Yang, X. Wang, A. Song, and S. Mao, "Wi-Wheat: Contact-free wheat moisture detection with commodity WiFi," in *2018 IEEE International Conference on Communications (ICC)*. IEEE, 2018, pp. 1–6.

[2] S. O. Nelson and S. Trabelsi, "Historical development of grain moisture measurement and other food quality sensing through electrical properties," *IEEE Instrumentation & Measurement Magazine*, vol. 19, no. 1, pp. 16–23, 2016.

[3] J. Ding and R. Chandra, "Towards low cost soil sensing using Wi-Fi," in *The 25th Annual International Conference on Mobile Computing and Networking*, 2019, pp. 1–16.

[4] L. Fan, Z. Chai, Y. Wang, Z. Wang, P. Zhao, J. Li, Q. Zhou, X. Qin, J. Yao, S. Yan *et al.*, "A novel handheld device for intact corn ear moisture content measurement," *IEEE Transactions on Instrumentation and Measurement*, vol. 69, no. 11, pp. 9157–9169, 2020.

[5] D. Cassanelli, N. Lenzini, L. Ferrari, and L. Rovati, "Partial least squares estimation of crop moisture and density by near-infrared spectroscopy," *IEEE Transactions on Instrumentation and Measurement*, vol. 70, pp. 1–10, 2021.

[6] Z. Wang, Y. Zhang, S. Fan, Y. Jiang, and J. Li, "Determination of moisture content of single maize seed by using long-wave near-infrared hyperspectral imaging (lwnir) coupled with uve-spa combination variable selection method," *IEEE Access*, vol. 8, pp. 195 229–195 239, 2020.

[7] W. Yang, E. Shen, X. Wang, S. Mao, Y. Gong, and P. Hu, "Wi-Wheat+: Contact-free wheat moisture sensing with commodity WiFi based on entropy," *Digital Communications and Networks*, 2022.

[8] W. Yang, X. Wang, S. Cao, H. Wang, and S. Mao, "Multi-class wheat moisture detection with 5GHz Wi-Fi: A deep LSTM approach," in *2018 27th International Conference on Computer Communication and Networks (ICCCN)*. IEEE, 2018, pp. 1–9.

[9] Y. Liu, L. Jiang, L. Kong, Q. Xiang, X. Liu, and G. Chen, "Wi-Fruit: See through fruits with smart devices," *Proceedings of the ACM on Interactive, Mobile, Wearable and Ubiquitous Technologies*, vol. 5, no. 4, pp. 1–29, 2021.

[10] J. A. Kong, *Electromagnetic Wave Theory*. EMW Publishing, 2005.

[11] R. v. Nee and R. Prasad, *OFDM for wireless multimedia communications*. Artech House, Inc., 2000.

[12] C. Wu, Z. Yang, Z. Zhou, K. Qian, Y. Liu, and M. Liu, "PhaseU: Real-time LOS identification with WiFi," in *2015 IEEE conference on computer communications (INFOCOM)*. IEEE, 2015, pp. 2038–2046.

[13] X. Wang, L. Gao, and S. Mao, "CSI phase fingerprinting for indoor localization with a deep learning approach," *IEEE Internet of Things Journal*, vol. 3, no. 6, pp. 1113–1123, 2016.

[14] P. Hu, W. Yang, X. Wang, S. Mao, and C. Niu, "WiPd: Contactless water-injected pork detection using commodity WiFi devices," in *Proc. IEEE MASS 2022*, Denver, CO, Oct. 2022, pp. 243–251.

[15] X. Wang, C. Yang, and S. Mao, "On CSI-based vital sign monitoring using commodity WiFi," *ACM Transactions on Computing for Healthcare*, vol. 1, no. 3, pp. 1–27, 2020.

[16] Z. Jiang and etc., "Picoscenes: Supercharging your next Wi-Fi sensing research!" https://ps.zpj.io/.

Authorized licensed use limited to: Auburn University. Downloaded on October 05,2023 at 15:34:47 UTC from IEEE Xplore. Restrictions apply.